Non-contact monitoring of glucose concentration and pH by integration of wearable and implantable hydrogel sensors with optical coherence tomography

MIMOZA NASESKA,[1,2] ALEŠ GLOBOČNIK,[1] SAMUEL DAVIES, [3] ALI K. YETISEN, [3] AND MATJAŽ HUMAR* [1,2,4]

[1]*Department of Condensed Matter Physics, J. Stefan Institute, Jamova 39, SI-1000 Ljubljana, Slovenia*
[2]*CENN Nanocenter, Jamova 39, SI-1000 Ljubljana, Slovenia*
[3]*Department of Chemical Engineering, Imperial College London, London SW7 2AZ, UK*
[4]*Faculty of Mathematics and Physics, University of Ljubljana, Jadranska 19, SI-1000 Ljubljana, Slovenia*
matjaz.humar@ijs.si

Abstract: Optical coherence tomography (OCT) is a noninvasive imaging technique with large penetration depth into the tissue, but limited chemical specificity. By incorporating functional co-monomers, hydrogels can be designed to respond to specific molecules and undergo reversible volume changes. In this study, we present implantable and wearable biocompatible hydrogel sensors combined with OCT to monitor their thickness change as a tool for continuous and real-time monitoring of glucose concentration and pH. The results demonstrate the potential of combining hydrogel biosensors with OCT for non-contact continuous in-vivo monitoring of physiological parameters.

1. Introduction

Hydrogels are loosely cross-linked water insoluble hydrophilic polymers that have the ability to absorb and retain water while maintaining their structure. The hydrogels investigated herein utilise a low crosslinking density which permits reversible changes to the swelling of polymer dependent on external stimuli [1]. By incorporating functional co-monomers into the polymer matrix, hydrogels can be designed to be sensitive to specific parameters in the environment. Functional co-monomers can bind biomarkers through their chemical functionality, leading to the production of a bound ionic charge within the hydrogel matrix. This bound ionic charge induces the movement of counter ions across the polymer membrane via Donnan osmotic pressure, resulting in swelling of the hydrogel. The relationship between biomarker and hydrogel expansion can be correlated and applied to numerous applications including tissue engineering and drug delivery [2]. There are several ways to detect the analyte of interest using swellable hydrogels such as photonic sensing of glucose [3], electrochemical identification of cholesterol [4] and visual quantification of Cu^{2+} ion concentration [5]. By implanting the biocompatible hydrogels [6] into the tissue they open the possibility of monitoring different physiological parameters, such as glucose or pH, depending on the hydrogel functionalization. However, the existing methods cannot be used subcutaneously, due to an inability to transduce biomarker detection through non-transparent tissue, requiring a different readout approach, and sensor biofouling [7].

Monitoring glucose levels is paramount for patients with diabetes. There are two types of devices intended for personal use and self-assessment of the glucose levels: non-continuous or self-monitoring blood glucose devices that monitor the glucose levels at specific points of the day and continuous glucose monitoring devices that automatically monitor glucose levels every few minutes making possible to record trends and observe rapid changes [8]. Currently, the most reliable devices on the market for continuous glucose monitoring measure glucose concentration in the interstitial fluid (ISF) [9], since ISF is the most prevalent fluid in the body that contains biomarkers that can provide information about cellular and tissue physiology [10].

Furthermore, they are not compatible with MRI and certain chemicals can interfere with the accuracy of readings such as paracetamol which can falsely elevate the glucose readings [11]. In such cases finger-prick tests are necessary to obtain accurate readings of glucose concentration. The invasive nature of these technologies is a key factor in poor adherence to testing regimes [12]. The development of a minimally invasive or non-invasive devices for glucose measurement would represent a life-changing factor for millions of patients around the world. There are several current and emerging technologies for glucose measurement [13] such as Raman spectroscopy [14], [15], mid-infrared [16], [17], photoacoustic spectroscopy [18], optical polarimetry [19], fluorescence glucose-sensing [20–22], nanomaterial-enhanced surface plasmon resonance [23] and several others which are at the beginning of their development [8].

Another physiological parameter monitored in healthcare is pH, which is important in many physiological processes like enzyme and tissue activities, blood gas saturation, angiogenesis during wound healing [24], collagen formation etc. [25]. Wound pH can be credible indicator of the state of the wound, since the patient's defense mechanisms change the local pH of a wound to affect microorganism invasion [25], [26]. Healthy skin pH varies from around 5 to 6 [27]. Upon injury pH rises to a more neutral value of the ISF (around 7.4) which is a result of the exposure of the underlying tissue to the environment. Variation can depend on wound severity with chronic wounds and infected wounds having neutral to alkaline pH (7.5 - 8.9) values [24]. Wounds with fungi or necrotic tissue have an acidic pH [28]. Monitoring pH of the wound may enable overview of the treatment response by providing information about bacterial or fungal contamination and improve the control over the healing process.

Optical coherence tomography is a non-invasive imaging technique based on low-coherence interferometry that uses infrared light and provides depth-resolved cross-sectional images of tissue [29]. In the past, there were attempts for using OCT alone for real time monitoring of glucose levels, due to its large penetration depth in tissue which can be up to 1 mm. However, OCT lacks sufficient chemical specificity. It was observed that temperature and several bodily osmolytes can change the refractive index of the tissue and significantly alter the measurements [17, 30]. There are several studies in the direction of enhancing OCT chemical specificity using glucose-sensing units [31–33]. In a recent study [33] hydrogel microparticles were used in which the submicron changes due to glucose were estimated from the OCT spectrum by modeling the microparticle as an optical cavity. In another study by R. Ballerstadt et al. [31] OCT was used to assess the turbidity of an implantable glucose sensor, but the specificity and accuracy of the sensor significantly decreased below the tissue due to the large attenuation of the OCT signal. S. Wang et al. [32] presented a glucose-sensing unit which contained a golden mirror. However, there were challenges with the precise placement of the sensor perpendicular to the laser beam and with maintaining the same scanning region on the sensor during multiple measurements.

Here we present the results of an investigation of the properties of tissue-implantable hydrogel-based biosensors for non-contact subcutaneous monitoring of glucose and pH-levels measured by using OCT. When combined with the implantable hydrogel biosensors, OCT can have high potential for continuous in-vivo monitoring of different physiological parameters.

2. Methods

Glucose sensitive hydrogel monomer solutions were prepared by photo cross-linking of acrylamide (AM, 73 mol%) and glucose-specific 3-acrylamido phenyl boronic acid (3-AAPB, 20 mol%) with 0.5 mol% methylene-bis-acrylamide (MBA) as a cross-linker and 2-hydroxy-2-methylpropiophenone (HMPP, 1 mol%), dissolved in a DMSO:H_2O (1:1, v/v) at a concentration of 0.5 g/mL as a photoinitiator [3]. The boronic acid group in 3-AAPB permits reversible covalent binding to glucose and functionnalizes the hydrogel. Boronic acid can exist in trigonal or tetrahedral form depending on the external conditions such as pH or temperature (see Fig. 1) [3].

The pH sensitive hydrogel was prepared by a free-radical polymerization of a hydrophylic monomer (hydroxyethyl)methacrylate (HEMA, 72 mol%) and a functional co-monomer dimethylaminoethyl acrylate (DMAEA, 25 mol%) and a crosslinker ethylene glycol dimethacrylate (EGDMA, 2 mol%) initiated by a photoinitiator 2-hydroxy-2-methylpropiophenone (HMPP, 1 mol%), diluted in propan-2-ol at a ratio of 1:1 [24]. The low crosslinking density of the pH responsive matrix allows for large volume variations depending upon the protonation and deprotonation of the functional co-monomer DMAEA which bears a tertiary amine and is capable of being protonated and deprotonated at different pH values. The reference hydrogel did not contain the boronic acid functional group. Most of the chemicals were obtained from Sigma Aldrich.

Both glucose and pH sensitive monomer solutions were prepared immediately prior to each hydrogel preparation to ensure reproducibility. The hydrogel films were prepared by pippetting of monomer solution on to the polyester side of aluminised film with glass microscope slides placed on top. It is imperative in the placing of the glass slide that no bubbles are within the liquid matrix prior to polymerisation. Samples were then polymerised via exposure to UV-A light for 30 min. Once fully polymerized the glass slide was soaked in warm water at 37^oC to detach the film. A small piece 1 mm^2 was cut off and put on a fresh glass slide. To measure the initial thickness the glucose-sensitive hydrogel sample was immersed into phosphate-buffered saline (PBS) at a constant pH 7.4. Solutions with different glucose concentrations were prepared by dissolving glucose in the PBS solution. The pH sensitive hydrogel film was equilibrated in a solution with pH 7. Solutions with different pH were prepared by dissolving appropriate amounts of HCl into 0.1 M TRIS buffer. To asses the response of the glucose or pH hydrogel sensors 500µL of fluid was used to cover the hydrogel placed on the glass slide. After waiting for about 20 min after immersion the hydrogel thickness was estimated. All measurements were conducted at room temperature.

OCT was used for hydrogel film thickness estimation. Wasatch Photonics Spectral-domain [29] OCT system (SPARK-HR800) was used in this study. It has an axial resolution of 3 µm in tissue, lateral resolution of 6 µm, imaging depth of 1.915 mm in air, A-scan line-rate of 70 kHz and a central wavelength of 846.2 nm. The thickness of the hydrogel was determined by hand using the Wasatch Photonics OCT software, SPARK OCT (version 2.1.5 9). The thickness was taken as the distance between the brightest pixels between the interfacial surfaces that represent the top and bottom surfaces of the hydrogel. To account for the subjectivity the reported thickness changes are the result of averaging. The hydrogel thickness was determined as an average of at least 4 points on the surface (B-scan). The error bars plotted on the graphs represent the statistical error.

The refractive index of the glucose-sensitive film for different glucose concentrations was measured with Abbe refractometer by using visible light.

For tissue measurements mouse skin was removed from the flank of the mouse. The glucose-sensitive film was placed on a glass slide between the mouse skin and a reference hydrogel film. As in the previous case all the test solutions were prepared using PBS.

To demonstrate the OCT visibility of the pH sensitive hydrogel below different coverings that are used to protect wounds we placed a small piece of pH-sensitive hydrogel film (25 mm^2) on a person's hand and finger and then covered the skin with an adhesive patch or with bandages. Afterwards an OCT B-scan was taken. The pH sensitive hydrogel film was equilibrated in a solution with pH 7 prior to measurements.

3. Results and Discussion

3.1. Subcutaneous glucose sensor

To test the glucose-sensitive hydrogels they were first placed on a glass slide, without any tissue and immersed into PBS. The hydrogel thickness varied between samples and it was between 100 and 150 µm. The films were transparent under optical microscope (Fig. 2a). A B-scan was

captured with the OCT (Fig. 2b). Top and bottom surfaces of the hydrogel film were nicely visible and enabled reliable determination of its thickness. The thickness was determined by measuring the film on at least 4 positions and the resulting error is displayed as error bars in all the plots. The OCT actually does not give the physical thickness, but rather the optical path length, which is the product of the geometric thickness and the refractive index. The refractive index of the hydrogel was measured for several different glucose concentrations. OCT measurements were done with near infrared light, while the refractive index was measured in visible light. Therefore, the dispersion curve of water, which is the main component of the hydrogel, was used to extrapolate the refractive index into the infrared range. The refractive index was also calculated from OCT B-scans. However due to the thickness error the resulting uncertainty of the refractive index was around 4% and was larger than the one obtained by the refractometer and extrapolation which was around 0.4% (Fig. 2c). The refractive index decreased with increasing glucose concentration (Fig. 2c) which is consistent with the fact that the hydrogel swells with increasing glucose concentration. The refractive index of the glucose solution is larger than pure water, and since this solution penetrates into the hydrogel it should have an opposite effect, that is an increase in the refractive index. However, the refractive index of 20 mM glucose at 550 nm is 1.334 only slightly higher compared to 1.333 of water. Therefore, this does not have a measurable effect.

The hydrogel swelling is a result of glucose association and dissociation with the boronic acid

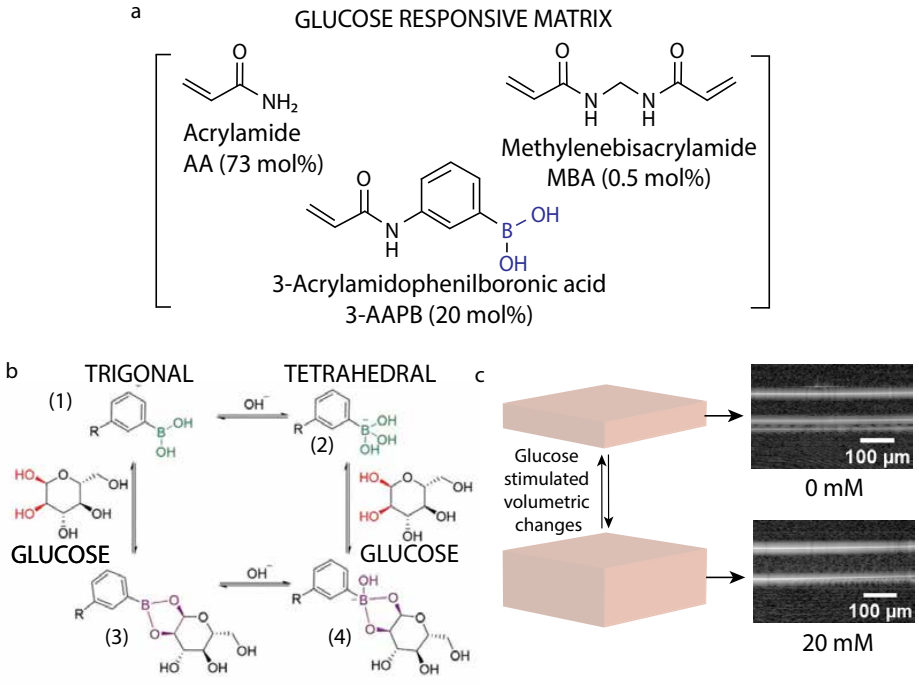

Fig. 1. a) Chemical structure of the glucose-sensitive hydrogel co-monomers. b) Reaction pathways for boronic acid binding of glucose in the trigonal and tetrahedral forms. Boronic acids can bind to glucose reversibly. At low pH, the boronic acid is trigonal planar form (1). This form does not readily complex with glucose, however it can form a strained complex (3). The strained form has a negative charge and it can be easily hydrolised. At higher pH the boronic acid is in a tetrahedral state (2) and it can bind to glucose more readily. c) Illustration (left) and OCT B-scan (right) of the glucose-induced volumetric changes on the hydrogel film.

in 3-AAPB forming a polymerized ionic charge (see Fig. 1). Boronic acid in 3-AAPB functions as a Lewis acid. 3-AAPB is trigonal and can react with water to form an anionic tetrahedral boronate. 1,2 ir 1,3 cis-diols of carbohydrates act as Lewis bases which can bind with boronic acis to form 5 or 6- membered cyclic boronate ester. This reaction depends on several factors such as pH, temperature and concentration [3].

The swelling was measured for concentrations of glucose in the interval from 0 to 20 mM with an increment of 2.5 mM. In all measurements the physical thickness of the hydrogel was calculated by taking into account the previously measured refractive index at each glucose concentration. In real life applications where an unknown concentration of glucose is measured, one cannot measure the physical thickness due to unknown refractive index. In that case the optical path length as measured by the OCT would be calibrated to the glucose concentration.

The initial thickness of the hydrogel film at zero glucose concentration (Fig. 2b) was 142 ± 0.2 µm. When immersed in a glucose solution it was observed that the hydrogel film thickness increased with the increasing glucose concentration until saturation (Fig. 2d). The subtle variations of the thickness as small as a few µm were clearly detectable with OCT. The largest response was in the range from 0 to 5 mM where the sensitivity was estimated to be 1.9%/mM and the detection limit was 0.7 mM. The detection limit was calculated as the product between the largest measured uncertainty in the thickness of the film and the slope of the line describing the thickness change in the glucose concentration interval from 0 to 5 mM. At larger intervals up to 10 mM the response was smaller, but still large enough for measuring concentration changes

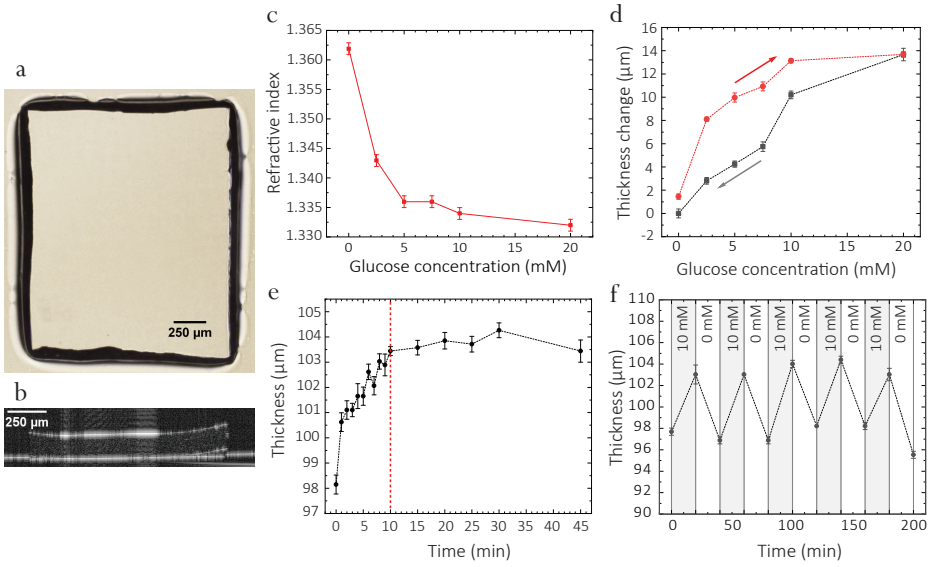

Fig. 2. Glucose-sensitive hydrogel film characteristics. a) Optical microscopy image in transmission of a hydrogel film sample placed on a glass slide. b) OCT B-scan revealing a cross-section image of the film. c) Increasing the glucose concentration resulted in decreasing the refractive index of the film. d) Hydrogel film thickness change as a response to increasing and decreasing glucose concentration. e) Time response of the hydrogel film. The curve was acquired by applying 10 mM glucose at time zero and measuring the thickness in time. The response time, marked with red dashed line, was defined as the time required for the thickness to reach 90% of the equilibrium swelling. f) Reversibility of the film thickness as a result of alternating glucose concentration with steps of 10 mM.

of the order of around 1.6 mM. When the glucose concentration was systematically decreasing from the maximal value a small hysteresis was observed (Fig. 2d) which appears because the decoupling of the glucose molecules from the boronic acid derivative is slower than the binding process [34].

The hydrogel film response time was defined as the time it takes for the swelling to reach 90% of the maximum value at a certain glucose concentration increment (in this case 10 mM) and it was estimated to be around 10 min. The measured response over almost one hour is shown in Fig. 2e. Due to rapid thickness changes within the first 10 min measurements were performed every minute. After around 15 min the thickness changes were negligible. The maximal swelling of

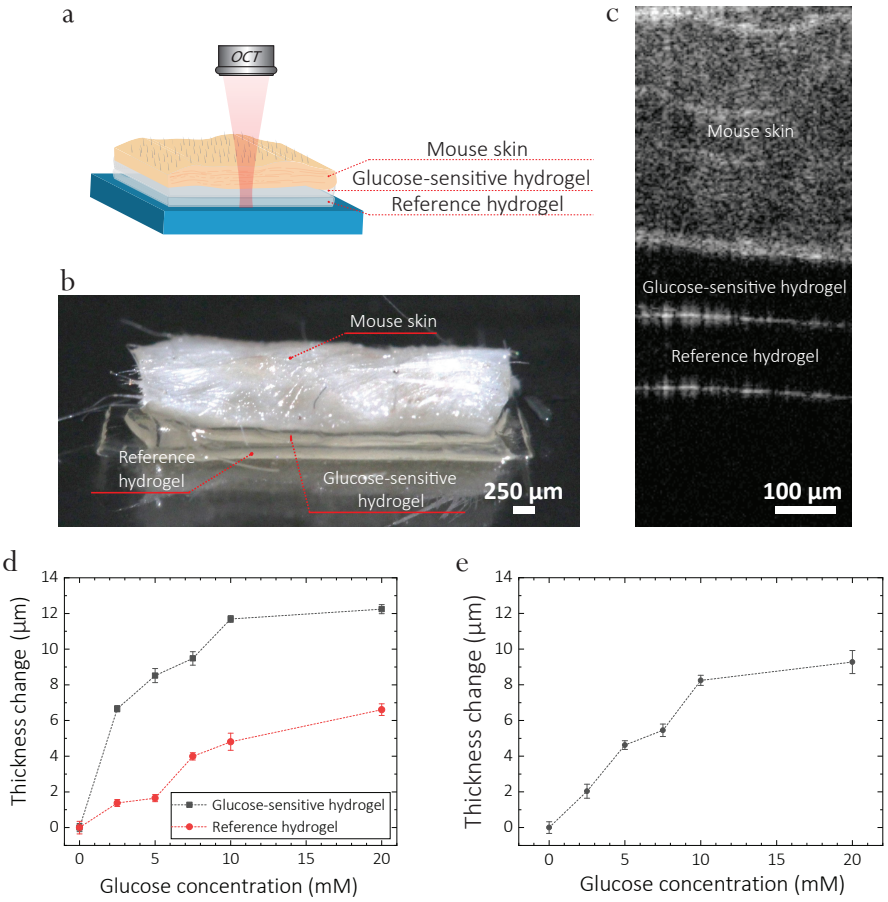

Fig. 3. Characterization of subcutaneous glucose sensor. a) Schematic illustration of the experimental setup. Glucose-sensitive hydrogel is placed between a mouse skin and a reference hydrogel which is significantly less sensitive to glucose. b) Photo of the measured sample. c) OCT B-scan which reveals a cross-section view. The 107 µm thick glucose-sensitive layer can be seen sandwiched between the mouse skin and the reference layer. d) A comparison between the response of the glucose-sensitive hydrogel film and the reference film measured separately by varying the glucose concentration. e) The hydrogel film was placed between the mouse skin and the reference hydrogel. Thickness change of the glucose-sensitive hydrogel film as a response to increasing glucose concentration.

the glucose-sensitive hydrogel film with thickness of 85 μm was measured to be around 12% in a glucose solution of 20 mM. For comparison, glucose concentration in the ISF can lag behind blood glucose concentration between 2 and 45 min [11]. Studies have suggested that the mean lag time is 6 to 7 min [35]. The measured response time was slightly shorter than reported for glucose-sensitive hydrogels in [33] and [36] which is in the range between 15 and 40 min.

To assess the robustness of the film, reversibility measurements were performed with alternating glucose concentrations of 0 and 10 mM (Fig. 1f). The hydrogel was observed to reversibly undergo swelling and deswelling over a number of cycles.

In table 1 we compare of the performance of the existing implantable glucose sensor studies for monitoring glucose using OCT. The range of glucose concentrations from 0 to 10 mM

Study	Modality	Compartment	Tests	Sens.	React. time	Detect. limit
S. Shah et al. [33]	OCT	ISF	in-vitro	2.4 %/mM	42 min	1.05 mM
R. Baller-stadt et al. [31]	OCT	ISF	in-vitro	0.74 %/mM	23 min	/
Our study	OCT	ISF	in-vitro	1.9 %/mM	10 min	0.7 mM

Table 1. Performance of tissue implantable glucose sensors for monitoring glucose using OCT.

corresponds to physiological levels from hypo- to normal to hyperglycaemic levels which means that the glucose-sensitive hydrogel can be used as a glucose-sensor for continuous subcutaneous monitoring of glucose levels in the whole physiological range. It is well known that there is a lag between glucose level changes in the ISF relative to the ones in the blood [35] and their values can differ within 10% [11]. In cases of hyperglycaemia peak glucose concentrations in the ISF lag behind blood glucose values. In this case the hydrogel reaction time and ISF lag time add up relative to the blood glucose values. However, in cases of hypoglycemia the ISF values fall before blood glucose values and in this case there can be no lag so the glucose value in the ISF can serve as a warning to prevent hypoglycemia [35]. The large sensitivity of the film in the hypoglicemic range can be advantageous and can be potentially used to warn the patient and prevent side-effects that can be very dangerous and in some specific situations even life-threatening.

The hydrogel biosensor can potentially be implanted in the dermis and imaged with an OCT in a non-contact mode. There are studies where ISF from the upper dermis was extracted and used for biomarker characterization [37], [10], [38]. In these studies small amounts of dermal ISF was extracted at depths between 250 μm and 700 μm and then analysed. By placing the sensor in the upper dermis in theory one can measure glucose concentration since it is estimated that there is 150 μL of ISF per cm^2 of human skin [39]. In theory this can be sufficient for our sensor to work properly (for a glucose film of around 1 mm^2 the minimal amount of glucose solution is around 150 μL). However, the amount of ISF is not equally distributed and there is larger amount in the lower dermis [10]. If one places the sensor at depths larger than 700 μm (lower dermis or hypodermis) one would need to use longer wavelengths for OCT imaging. At 1600 nm, for

example, it is estimated that the penetration depth in tissue can reach several mm, but scattering and water content can be an important factor for scan quality.

As a proof of concept we tested the performance of the glucose sensor under a mouse skin by measuring its response in different glucose concentrations. The skin had thickness of approximately 300 μm as estimated from the OCT scans. The schematics and the results of the experiment are shown in Fig. 3. The response of the reference film in comparison to the glucose-sensitive hydrogel is shown in Fig. 3d. When placed between the reference layer and the mouse skin the hydrogel film glucose sensitivity decreased and the maximal swelling measured was around 7.4% in a glucose solution of 20 mM. In comparison, the swelling of the hydrogel not embedded below a piece of skin (Fig 3d) was around 12 % in the same conditions. This suggests that the layer of skin above the hydrogel sensor might cause a mechanical stress which can have an influence on its sensing properties. In some situations this can be compensated for by the reference film. The reference film did not have the glucose sensing capability and was located below the glucose sensitive film (see FIg. 3c). Measurements show that the reference hydrogel film had significantly smaller sensitivity to glucose in comparison to the glucose-sensitive hydrogel (Fig. 2d). Any other environmental change such as mechanical stress and pH would also influence the reference film. Since the two films are collocated, any such thickness change can be then subtracted from the glucose sensitive film. In this way it would be possible to cancel out the other influences, leaving only the contribution due to glucose.

3.2. Wearable pH sensor

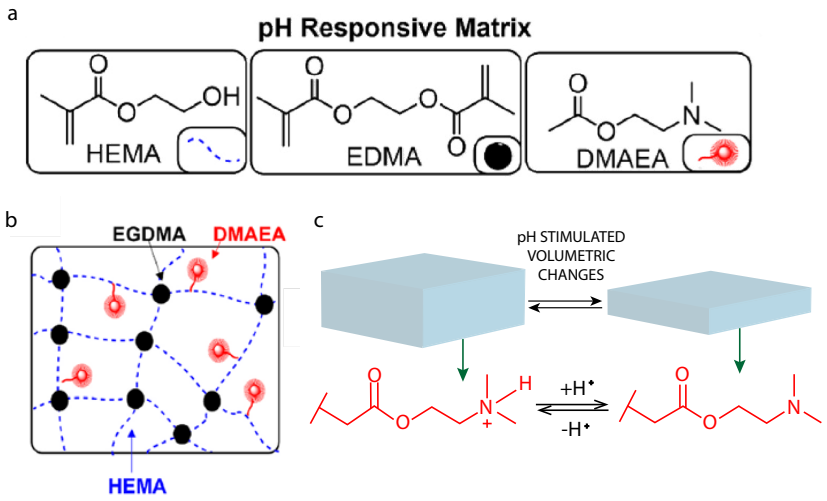

Fig. 4. pH-sensitive hydrogel chemistry. a) Schematic illustration of the co-monomer chemical structure and hydrogel framework b). The functional co-monomer DMAEA allows for volumetric changes of the hydrogel film upon changing the pH of the solution c).

The response of the pH-sensitive hydrogel film was measured in solutions with pH in the interval from 7 to 9. The low crosslinking density of the pH responsive matrix allows for large volume variations depending upon the protonation and deprotonation of the functional co-monomer DMAEA which bears a tertiary amine and is capable of being protonated and deprotonated at different pH values (Fig 4). The level of protonation is dependent on the acidic dissociation constant (pK_a) of the amines lone pair of electrons and their ability to donate electron

density to protons within a solution. [24].

The hydrogel film thickness decreases with the increasing pH of the solution (Fig. 5). The value of the film thickness was calculated from OCT cross-sections by taking a fixed refractive index of 1.34 [24]. The maximal thickness change was 21% when changing the pH from 7 to 9. The pH-sensitive hydrogel has a large sensitivity in the interval from pH 7 to pH 9 which are values that are important in healthcare. Upon injury wound pH is around 7.4 and variations can differ depending upon wound severity in the range from neutral to alkaline (7.5 to 8.9) values [24]. The pH-sensitive hydrogel can offer the possibility of non-contact monitoring of

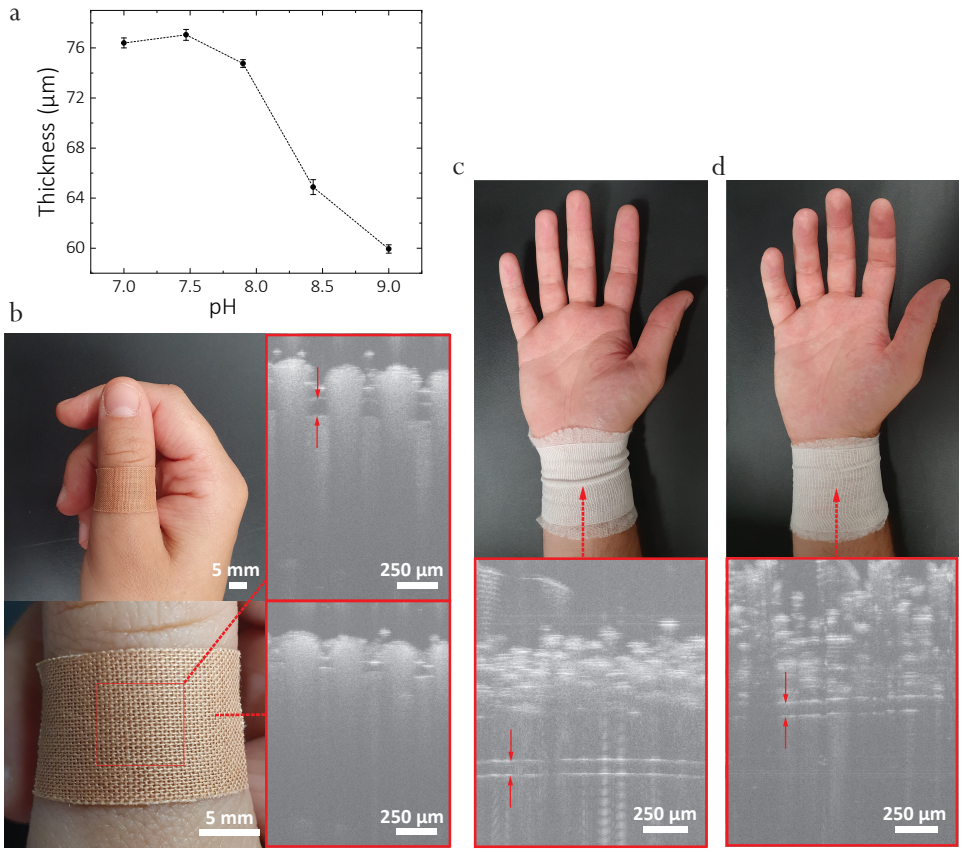

Fig. 5. pH-sensitive hydrogel film for wound monitoring. a) The graph shows the deswelling of the film as a response to increasing pH of the solution. b) OCT B-scan of the hydrogel film located below a finger patch (upper right) and of the surrounding area with no hydrogel film (lower right). The arrows on the top right image indicate the location of the hydrogel film. The upper left image shows the location of the patch and the rectangle on the lower left image indicates the location of the hydrogel film. c) OCT B-scan of the pH sensitive film located below one layer of gauze and one layer of bandage, shown on the photo. The arrows indicate the location of the hydrogel film which is clearly visible on the OCT scan. d) OCT B-scan of the pH sensitive film located below two layers of gauze and one layer of bandage. The arrows indicate the location of the hydrogel film. The increasing number of covering layers reduces the visibility of the hydrogel under OCT.

the wound pH. OCT images of the hydrogel placed below an adhesive patch and below two and

three layers of bandage (Fig. 5) clearly reveal its visibility that can be sufficient to estimate its thickness and consequently obtain an information about the wound pH. Characterization of the wound non-contactly would allow for continuous monitoring of the healing progression without each time removing the bandages which can cause additional trauma. With the current measurement range monitoring until healing is not possible since healing occurs in more acidic environment where the sensitivity of the film is almost non-existent [24], however early detection of pathological developments is possible and would enable prompt therapeutic intervention. In the other cases one can use a hydrogel with a lower pH measurement range. pH-sensitive hydrogels would also allow for a more objective approach in wound characterization since currently the wound management relies mainly on visual evaluation and subjective assessment.

4. Conclusions

We have shown that OCT combined with bio-compatible glucose-sensitive hydrogel implanted subcutaneously can have potential for minimally invasive continuous and real-time monitoring of glucose levels. We have also shown that OCT has the possibility of non-contact wound characterization when combined with pH-sensitive hydrogel film placed in contact with the wound. The use of analyte-specific swellable hydrogels allows for chemical specificity in OCT imaging.

The proof of concept for monitoring glucose concentration looks promising and with some improvements in the hydrogel properties it can be used for practical applications. Additional information about selectivity, specificity and LOD of the hydrogels can be found in [3], [24], [40], [34] and [41]. For example, currently available glucose-monitors have response time in the order of few minutes at most and the glucose-levels in the body can change on a timescale less than a minute. This means that fast-acting hydrogels will be important improvement. In the case of wound monitoring, hydrogels with larger pH sensitivity can enable non-contact observation of wounds until healing. Future work directed into improving the materials that are currently used for sensing [35] and on modifying the detection system can allow production of a wearable devices that can be easily used by the patients.

Here, we choose planar geometry for the hydrogel sensors, however other geometries, such as spheres [33] or fibers could also be employed. The planar geometry however offers some advantages. Firstly, having a hydrogel layer allows measurements of the thickness change on several different spots making the measurement more accurate and compensate for irregularities.

Secondly, having multiple layers allows the measurement of several parameters simultaneously. Even though the measurements were done on stacked layers placing the layers side by side allows for better visibility and more accurate measurements of the additional parameters, since both layers will be in a similar mechanical and chemical environment.

Thirdly, by having a non-responsive reference hydrogel any thickness change due to mechanical forces can be compensated for. In the case of spheres and fibers it would be possible to measure both the diameter and the refractive index by measuring vertical and horizontal dimension, however with a strong assumption that the cross section is perfectly spherical. But due to possible mechanical deformation it is then impossible to distinguish the deformation from swelling and refractive index change.

In future, the method developed here could be further extended to other biomarkers through the utilisation of alternative co-monomers such as crown ligands for ionic species or through molecular imprinting for drug and protein detection. By further developments in miniaturizing OCT system, such as in multiple reference optical coherence tomography (MR-OCT) [42], which is small, robust and low cost, one can bring the use of OCT closer to consumers and enable the development of personalized medicine through wearable devices similar to smart watches based on OCT technology. The greater collection of data in point of care settings through such technology permits more regular testing to obtain real time information of patient wellbeing. This

not only benefits immediate treatment with tailoring of care to the current patient requirements, but also expands the information available to medical researchers about potential early warning signs of illness which are currently unknown and which could revolutionise medical systems globally.

Acknowledgments

This project has received funding from the European Research Council (ERC) under the European Union's Horizon 2020 research and innovation programme (grant agreement No. 851143) and from Slovenian Research Agency (ARRS) (P1-0099).

Competing interests

The authors declare no competing interests.

Data availability

All data that support the plots within this paper and other findings of this study are available from the corresponding author upon reasonable request.

References

1. N. V. Gupta and H. Shivakumar, "Investigation of swelling behavior and mechanical properties of a pH-sensitive superporous hydrogel composite," Iran. J. Pharm. Res. **11**, 481 (2012).
2. Y. Qiu and K. Park, "Environment-sensitive hydrogels for drug delivery," Adv. Drug Deliv. Rev. **53**, 321–339 (2001).
3. S. Davies, Y. Hu, J. Blyth, *et al.*, "Reusable dual-photopolymerized holographic glucose sensors," Adv. Funct. Mater. **33**, 2214197 (2023).
4. L. Li, Y. Wang, L. Pan, *et al.*, "A nanostructured conductive hydrogels-based biosensor platform for human metabolite detection," Nano Lett. **15**, 1146–1151 (2015).
5. R. Wu, S. Zhang, J. Lyu, *et al.*, "A visual volumetric hydrogel sensor enables quantitative and sensitive detection of copper ions," Chem. Commun. **51**, 8078–8081 (2015).
6. F. A. Andersen, "Amended final report on the safety assessment of polyacrylamide and acrylamide residues in cosmetics," Int. J. Toxicol. **24**, 21–50 (2005).
7. J. Xu and H. Lee, "Anti-biofouling strategies for long-term continuous use of implantable biosensors," Chemosensors **8**, 66 (2020).
8. W. Villena Gonzales, A. T. Mobashsher, and A. Abbosh, "The progress of glucose monitoring—a review of invasive to minimally and non-invasive techniques, devices and sensors," Sensors **19**, 800 (2019).
9. V. D. Funtanilla, T. Caliendo, and O. Hilas, "Continuous glucose monitoring: a review of available systems," Pharm. Ther. **44**, 550 (2019).
10. P. P. Samant, M. M. Niedzwiecki, N. Raviele, *et al.*, "Sampling interstitial fluid from human skin using a microneedle patch," Sci. translational medicine **12**, eaaw0285 (2020).
11. R. Lin, F. Brown, S. James, *et al.*, "Continuous glucose monitoring: a review of the evidence in type 1 and 2 diabetes mellitus," Diabet. Med. **38**, e14528 (2021).
12. S. Laha, A. Rajput, S. S. Laha, and R. Jadhav, "A concise and systematic review on non-invasive glucose monitoring for potential diabetes management," Biosensors **12**, 965 (2022).
13. I. Ahmed, N. Jiang, X. Shao, *et al.*, "Recent advances in optical sensors for continuous glucose monitoring," Sens. Diagn. **1**, 1098–1125 (2022).
14. A. Pors, K. G. Rasmussen, R. Inglev, *et al.*, "Accurate post-calibration predictions for noninvasive glucose measurements in people using confocal raman spectroscopy," ACS sens. **8**, 1272–1279 (2023).
15. Q. Wang, D. Sun, X. Ma, *et al.*, "Surface enhanced raman scattering active substrate based on hydrogel microspheres for pretreatment-free detection of glucose in biological samples," Talanta **260**, 124657 (2023).
16. J. Sa, Y. Song, H. Gu, and Z. Zhang, "Mid-infrared spectroscopy with an effective variable selection method based on mpa for glucose detection," Chemom. Intell. Lab. Syst. **233**, 104731 (2023).
17. S. Liakat, K. A. Bors, L. Xu, *et al.*, "Noninvasive in vivo glucose sensing on human subjects using mid-infrared light," Biomed. Opt. Express **5**, 2397–2404 (2014).
18. M. R. Kaysir, J. Song, S. Rassel, *et al.*, "Progress and perspectives of mid-infrared photoacoustic spectroscopy for non-invasive glucose detection," Biosensors **13**, 716 (2023).
19. R. Rawer, W. Stork, and C. F. Kreiner, "Non-invasive polarimetric measurement of glucose concentration in the anterior chamber of the eye," Graefe's Arch. Clin. Exp. Ophthalmol. **242**, 1017–1023 (2004).
20. D. C. Klonoff, "Overview of fluorescence glucose sensing: a technology with a bright future," J. diabetes Sci. Technol. **6**, 1242–1250 (2012).

21. C. Chen, X.-L. Zhao, Z.-H. Li, *et al.*, "Current and emerging technology for continuous glucose monitoring," Sensors **17**, 182 (2017).
22. L. Colvin, D. Tu, D. Dunlap, *et al.*, "A polarity-sensitive far-red fluorescent probe for glucose sensing through skin," Biosensors **13**, 788 (2023).
23. S. Zeng, D. Baillargeat, H.-P. Ho, and K.-T. Yong, "Nanomaterials enhanced surface plasmon resonance for biological and chemical sensing applications," Chem. Soc. Rev. **43**, 3426–3452 (2014).
24. S. Davies, Y. Hu, N. Jiang, *et al.*, "Reversible photonic hydrogel sensors via holographic interference lithography," Biosens. Bioelectron. **207**, 114206 (2022).
25. Z. Zulkarnay, S. Shazwani, B. Ibrahim, *et al.*, "An overview on pH measurement technique and application in biomedical and industrial process," in *2015 2nd International Conference on Biomedical Engineering (ICoBE),* (IEEE, 2015), pp. 1–6.
26. S. L. Percival, S. McCarty, J. A. Hunt, and E. J. Woods, "The effects of pH on wound healing, biofilms, and antimicrobial efficacy," Wound Repair Regen. **22**, 174–186 (2014).
27. M.-H. Schmid-Wendtner and H. C. Korting, "The ph of the skin surface and its impact on the barrier function," Ski. Pharmacol. Physiol. **19**, 296–302 (2006).
28. L. A. Schneider, A. Korber, S. Grabbe, and J. Dissemond, "Influence of ph on wound-healing: a new perspective for wound-therapy?" Arch. Dermatol. Res. **298**, 413–420 (2007).
29. Z. Yaqoob, J. Wu, and C. Yang, "Spectral domain optical coherence tomography: a better OCT imaging strategy," BioTechniques **39**, S6–S13 (2005).
30. K. V. Larin, T. V. Ashitkov, M. Motamedi, and R. O. Esenaliev, "Specificity of noninvasive blood glucose monitoring with optical coherence tomography," in *Optical Diagnostics and Sensing in Biomedicine III,* vol. 4965 (SPIE, 2003), pp. 25–31.
31. R. Ballerstadt, A. Kholodnykh, C. Evans, *et al.*, "Affinity-based turbidity sensor for glucose monitoring by optical coherence tomography: Toward the development of an implantable sensor," Anal. Chem. **79**, 6965–6974 (2007).
32. S. Wang, T. Sherlock, B. Salazar, *et al.*, "Detection and monitoring of microparticles under skin by optical coherence tomography as an approach to continuous glucose sensing using implanted retroreflectors," IEEE Sens. J. **13**, 4534–4541 (2013).
33. S. Shah, C.-N. Yu, M. Zheng, *et al.*, "Microparticle-based biochemical sensing using optical coherence tomography and deep learning," ACS Nano **15**, 9764–9774 (2021).
34. A. K. Yetisen, Y. Montelongo, F. da Cruz Vasconcellos, *et al.*, "Reusable, robust, and accurate laser-generated photonic nanosensor," Nano lett. **14**, 3587–3593 (2014).
35. N. Oliver, C. Toumazou, A. Cass, and D. Johnston, "Glucose sensors: a review of current and emerging technology," Diabet. Med. **26**, 197–210 (2009).
36. M. Bajgrowicz-Cieslak, Y. Alqurashi, M. I. Elshereif, *et al.*, "Optical glucose sensors based on hexagonally-packed 2.5-dimensional photonic concavities imprinted in phenylboronic acid functionalized hydrogel films," RSC Adv. **7**, 53916–53924 (2017).
37. M. Friedel, I. A. Thompson, G. Kasting, *et al.*, "Opportunities and challenges in the diagnostic utility of dermal interstitial fluid," Nat. Biomed. Eng. pp. 1–15 (2023).
38. B. Q. Tran, P. R. Miller, R. M. Taylor, *et al.*, "Proteomic characterization of dermal interstitial fluid extracted using a novel microneedle-assisted technique," J. proteome research **17**, 479–485 (2018).
39. P. P. Samant and M. R. Prausnitz, "Mechanisms of sampling interstitial fluid from skin using a microneedle patch," Proc. National Acad. Sci. **115**, 4583–4588 (2018).
40. A. K. Yetisen, N. Jiang, A. Fallahi, *et al.*, "Glucose-sensitive hydrogel optical fibers functionalized with phenylboronic acid," Adv. mater. **29**, 1606380 (2017).
41. M. Elsherif, F. Alam, A. E. Salih, *et al.*, "Wearable bifocal contact lens for continual glucose monitoring integrated with smartphone readers," Small **17**, 2102876 (2021).
42. M. Leahy, J. Hogan, C. Wilson, *et al.*, "Multiple reference optical coherence tomography (MR-OCT) system," in *Dynamics and fluctuations in biomedical photonics X,* vol. 8580 (SPIE, 2013), pp. 59–66.